

Innovative integrated process for the treatment of azo dyes: coupling of photocatalysis and biological treatment

S. Brosillon, H. Djelal, N. Merienne, A. Amrane*

UMR CNRS 6226 SCR, Equipe Chimie et Ingénierie des Procédés, ENSCR — Université de Rennes 1,
ENSCR, Avenue du Général Leclerc, 35700 Rennes, France
email: abdeltif.amrane@univ-rennes1.fr

Received 17 December 2006; accepted 3 January 2007

Abstract

Tests of the biodegradation of the azo dyes Reactive Black 5 and Reactive Yellow 145 confirmed the low biodegradability of these components in the considered conditions, namely a strain of *Pseudomonas fluorescens*, cultivated at 25°C, an initial pH of 7 and in presence of a supplementary carbon source, glucose. Indeed, for an initial dye concentration of 40 ppm, the maximum yields of decolouration were 27% and 18% for the two dyes RB5 and RY145. Some tests of biological mineralisation of solutions preliminarily photocatalysed demonstrate a mineralisation of the considered solutions for various irradiation times. Identification of the intermediate by-products is in progress to propose a reaction pathway.

Keywords: Azo dyes; Biodegradation; Integrated processes; Photocatalysis

1. Introduction

Tannery factories are important user of dyes, an important source of pollution, especially in some countries, high leather producers, like China and North African countries. Processes for the treatment of heavy metals, like chromium or cadmium, which often accompanies dyes, are now well known and controlled. Owing to their colouration, the dyes cause floral pollution and aesthetic pollution (even a small amount of dye is clearly

apparent). However, even if dyes are not toxic, the toxicity of their by-products has to be considered. Indeed, dyes degradation led to aromatic amines, which are known to be toxic.

Among the advanced oxidative processes (AOP), heterogeneous photocatalysis appears as an interesting technique for the treatment of endogenic organic pollutions [1–3]. Indeed, titan dioxide (TiO₂) activation under UV irradiation ($\lambda < 390$ nm) allows the generation from water or hydroxide ions of free radicals •OH, highly reactive. These free radicals can then react with the persistent components adsorbed at the surface

*Corresponding author.

Presented at the conference on Desalination and the Environment. Sponsored by the European Desalination Society and Center for Research and Technology Hellas (CERTH), Sani Resort, Halkidiki, Greece, April 22–25, 2007.

of titan dioxide until their total mineralisation. The ambient temperature and the possible use of solar UV are the photocatalysis advantages; moreover titan dioxide is not toxic.

A long period of time can be required for the disappearance of the active molecule and its complete mineralisation during photocatalytic degradation. Moreover, there is a lack in the knowledge concerning the different steps of the mineralisation and the formed by-products. Therefore, the integration of two processes, photocatalysis and biological treatment can be helpful, in order to reduce the costs. The use in the laboratory of TiO₂ coated on a non-woven cellulose fiber is interesting, since it allows to remove the tedious filtration step of catalyst [4]. The reaction pathway and the photocatalytic kinetic degradation have to be better known in view of the optimisation of the operating conditions of the integrated process (irradiation time, mineralisation yield, etc.).

The main mechanism of azo dye degradation is its adsorption on activated sludge [5]. However, some bacterial strains show the ability to degrade azo dyes by breaking the azoic bond under aerobic conditions, leading to a high degradation level, as shown with a strain of *Enterobacter agglomerans* [6]. Azoic dyes biodegradation can also be carried out under microaerophilic conditions [7]. Anaerobic conditions also lead to the rupture of the azoic bond [8,9], leading to the colour disappearance. However, anaerobic conditions lead to incomplete mineralisation; toxic and carcinogenic by-products can result from the cleavage of the azoic bond [10]. Indeed, aromatic amines are obtained, which are difficult to treat, owing to their high stability under anaerobic conditions.

The non-specific nature of the azoic reduction has been shown by several authors [9,11]. A non-specific reaction between azo dyes and reduced flavins resulting from flavin reductases has been proposed. An increase of the reduction rate, namely an increase of the treatment process result from the use of these flavin reductases [9,12]. Biomass uses for its growth not only the nitrogen content

of azo dye, but can also use its carbon content. However, growth yield can be improved by adding a primary carbon source, like glucose [13].

Organic compounds derived from hydrocarbons, from chlorinated, phosphate or sulphur compounds, as is the case for the considered azo dyes, can be, at least partially, degraded by enzymes expressed by *Pseudomonas* species [14]. The efficiency of the biodegradation of organic compounds, like hydrocarbons, varied with the structure of the molecule (linear or ramified, aliphatic or aromatic). During biodegradation, organic compounds mineralisation by bacteria leads to carbon dioxide and water. Among the microorganisms involved in environmental applications, *P. fluorescens* was chosen since this species is not pathogenic and not dangerous for the environment in proportion to its large use in xenobiotic bioremediation.

Combining processes have been proposed to treat wastewater generated by the textile industry and containing among other dyes, including UV/H₂O₂ or UV/O₃ [15] or photo-fenton UV/Fe³⁺/H₂O₂ [16] followed by biological treatment. The degradation of a biorecalcitrant dye precursor was also examined in an integrated Fe(III) photoassisted-biological reactor without addition of other electron acceptor than O₂ [17] and in a coupled solar-biological system which allowed to compare four commonly used photoassisted advanced oxidation process (AOP) [18]. Mineralisation of azo dyes was also examined in a two stage sequential Fenton's oxidation followed by aerobic biological treatment [19]. Indeed, potential advantages of the strategy of combining chemical and biological processes to treat contaminants in wastewater was previously suggested [20,21].

In this paper are therefore presented preliminary results concerning the degradation of two azo dyes Reactive Black 5 (RB5) and Reactive Yellow 145 (RY145) used in Moroccan tannery factories by means of an integrated process involving photocatalysis UV/TiO₂ followed by biological treatment.

2. Materials and methods

2.1. Azo dyes

The two dyes, RB5 and RY145, were purchased from the Moroccan textile industry and used without further purification. The molecular structure of each dye is given in Fig. 1. Purified water (Elix Millipore equipment) was used to prepare the coloured solutions.

2.2. Microorganism

A commercial strain of *P. fluorescens* Migula 1895^{AL} (DSMZ, Braunschweig, Germany) was used. Stock cultures were maintained on the following medium (g L⁻¹): glucose (Merck, Darmstadt, Germany), 10, yeast extract (Biokar Diagnostics/Solabia, Pantin, France), 15, and glycerol (Merck), 200; and deep-frozen at -20°C.

2.3. Culture media

Preculture medium contained (g L⁻¹): glucose, 20, pancreatic casein peptone (Biokar), 20, yeast extract, 10. Medium pH was then adjusted to 7

with 1 M NaOH, before it was sterilised at 121°C for 20 min.

Culture medium contained the considered azo dye, 40 mg L⁻¹, ammonium (Merck), 0.9 g L⁻¹ (namely 50 mmol L⁻¹ NH₄Cl) and the following mineral supplementation: inorganic phosphates, 25 mmol L⁻¹ of KH₂PO₄ and 25 mmol L⁻¹ of NaH₂PO₄, H₂O, as well as a solution of EDTA (ethylene-diamine-tetra-acetate) (584 mg L⁻¹) chelated trace elements (mg L⁻¹) [22]: Mg, 25; Fe, 20; Ca, 18; Zn, 4.5; Mo, 2; Cu, 1.3. As for preculture medium, pH was then adjusted to 7, before the medium was sterilised.

When needed, and after sterilisation to avoid coloured Maillard reaction, glucose was added to the culture medium at the required concentration, namely in the range 0–2 g L⁻¹.

2.4. Culture conditions

Bacteria were precultivated during 12–15 h at 37°C in 100 mL Erlenmeyer flasks, containing 50 mL of working volume. Culture medium was inoculated with 3 mL seed culture; then carried out in 250 mL Erlenmeyer flasks containing

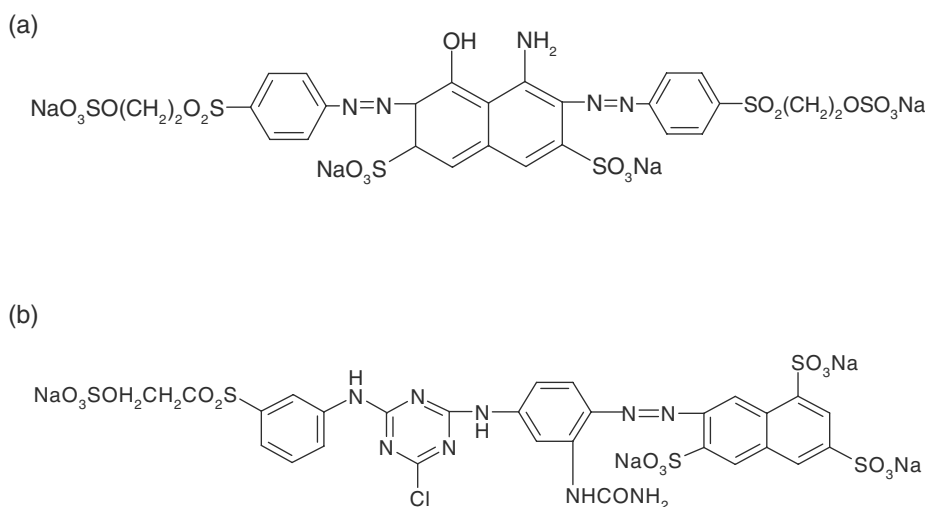


Fig. 1. Reactive Black 5 (RB5) (a) and Reactive Yellow 145 (RY145) (b) chemical structures. RB5 class: diazo; reactive group: sulfatoethylsulfone; natural pH: 5.8; λ_{\max} : 597 nm; molecular weight: 991.8 g mol⁻¹. RY145 class: diazo; reactive group: sulfatoethylsulfone; natural pH: 5.9; λ_{\max} : 419 nm; molecular weight: 1026.2 g mol⁻¹.

120 mL of medium. Flasks were incubated at 30°C on a rotary shaker at 350 rpm agitation speed. Experiments were conducted in duplicate.

2.5. Photocatalyst characteristics

The powdered photocatalyst was PC-500 Titania from Millennium Inorganic Chemicals (anatase > 99%; specific surface area > 320 m² g⁻¹; crystallites mean size: 5–10 nm, characteristics from Millenium Chemicals company). Titania PC-500 was also coated on non-woven paper (natural cellulose fiber, 2 mm thick) using a binder. The binder was an aqueous dispersion of colloidal SiO₂. The cellulose fiber is coated by a mixture of TiO₂ and SiO₂ (particle size 20–30 nm; TiO₂/SiO₂ mass ratio: (1) using a size press. The TiO₂ surface load was 25 g m⁻² after washing. In this study, the combination cellulose fiber–TiO₂–SiO₂ will be referred to as the photocatalytic medium.

2.6. Photoreactor and light source

Irradiations were performed in a cylindrical batch reactor (volume: $V = 4$ L, diameter: $\varnothing = 18$ cm), fitted with a 25 W low-pressure fluorescent lamp (Philips PL-L 24W/10/4P, maximal emission wavelength 365 nm) vertically placed in a plugged tube. A quartz cylindrical jacket located around the plugging tube contained circulating water at constant temperature to avoid heating of the solution. The cylindrical reactor was placed in a thermostated tank at 25°C. In a typical experiment, the photocatalytic media was fixed on the inner wall of the photoreactor (surface: 0.112 m², corresponding to 2.80 g of TiO₂). The water thickness between the quartz jacket and the inner wall was 0.05 m. The radiant flux received by the solution was measured by means of a chemical actinometer (potassium ferrioxalate). The actinometer was irradiated under similar conditions as the experimental conditions used during the degradation studies. The incident photon flux, P_0 , was estimated to $(8.1 \pm 0.1) 10^{-6}$ Einstein s⁻¹,

corresponding to (18.6 ± 0.2) W m⁻² at the reactor's inner wall.

2.7. Photocatalysis conditions

Four liters of solution containing 80 mg L⁻¹ azo dye were introduced into the photoreactor. The solution was mixed in the reactor by means of an impeller. Atmospheric dried air pressured was introduced through a bubbler. Photocatalysis reaction was carried out until the required percentage of discolouration was achieved, namely 25% (IR25), 50% (IR50) and 100% (IR100) of dye degradation.

2.8. Analyses

In a typical photocatalysis experiment, at scheduled times, 5 mL of sample were taken from the reactor and filtered through a Millipore filter (Millex[®]-HV, 0.45 μm). Photocatalysis reaction was followed by UV–Vis spectra using a Cary 50 (190–1100 nm) spectrophotometer. The kinetics of the reaction was monitored measuring the absorbance at $\lambda = 419$ and 597 nm for RB5 and RY145 respectively [23], found to be the wavelength giving the maximum of absorption.

During culture, pH was monitored, as well as bacterial growth [24] turbidimetrically followed after periodical sampling at a wavelength of 600 nm, using a Thermospectronic Helios 8 spectrophotometer (Bioblock, Illkirch, France). The remaining analyses were then carried out after centrifugation of samples (20 min at 4000 rpm — Jouan C412, Saint-Herblain, France). The kinetics of dye biodegradation were monitored measuring the absorbance at $\lambda = 419$ and 597 nm for RB5 and RY145, respectively. Glucose and ammonium were determined by the phenol–sulphuric acid method for total sugars [25] and the Nessler method (NF t 90-015 standard [26]), respectively. Total organic carbon (TOC) measurements were carried out by means of a 1010 O.I. Analytical TOC analyzer, after filtration through a Millipore

filter (Millex®-HV-0.45 μm) to totally avoid particles entering the TOC apparatus.

3. Results and discussion

3.1. Biodegradation essays

Fig. 2a shows high initial turbidity of the culture medium containing RB5 dye. Indeed, from the absorbance spectrum of RB5 [27], it appears that this dye highly absorbed in the wavelength range 500–650 nm, for which turbidity was shown to vary in proportion to dry cellular weight (total biomass) for a useful range of concentrations [28].

Contrarily, at 600 nm there was no absorption of RY145 (not shown), leading to low values for the initial turbidity of the culture medium (Fig. 2b).

However, irrespective of the presence or not of an additional carbon source in the culture medium, like glucose, the increase of the turbidity recorded during growth on medium containing RB5 was higher than that recorded on medium containing RY145, namely in the range 0.77–1.07 and 0.49–0.75 respectively, for glucose concentrations in the range 0–2 g L⁻¹. For both dyes, in absence of glucose or for 1 g L⁻¹ glucose in the culture medium, turbidity increased throughout

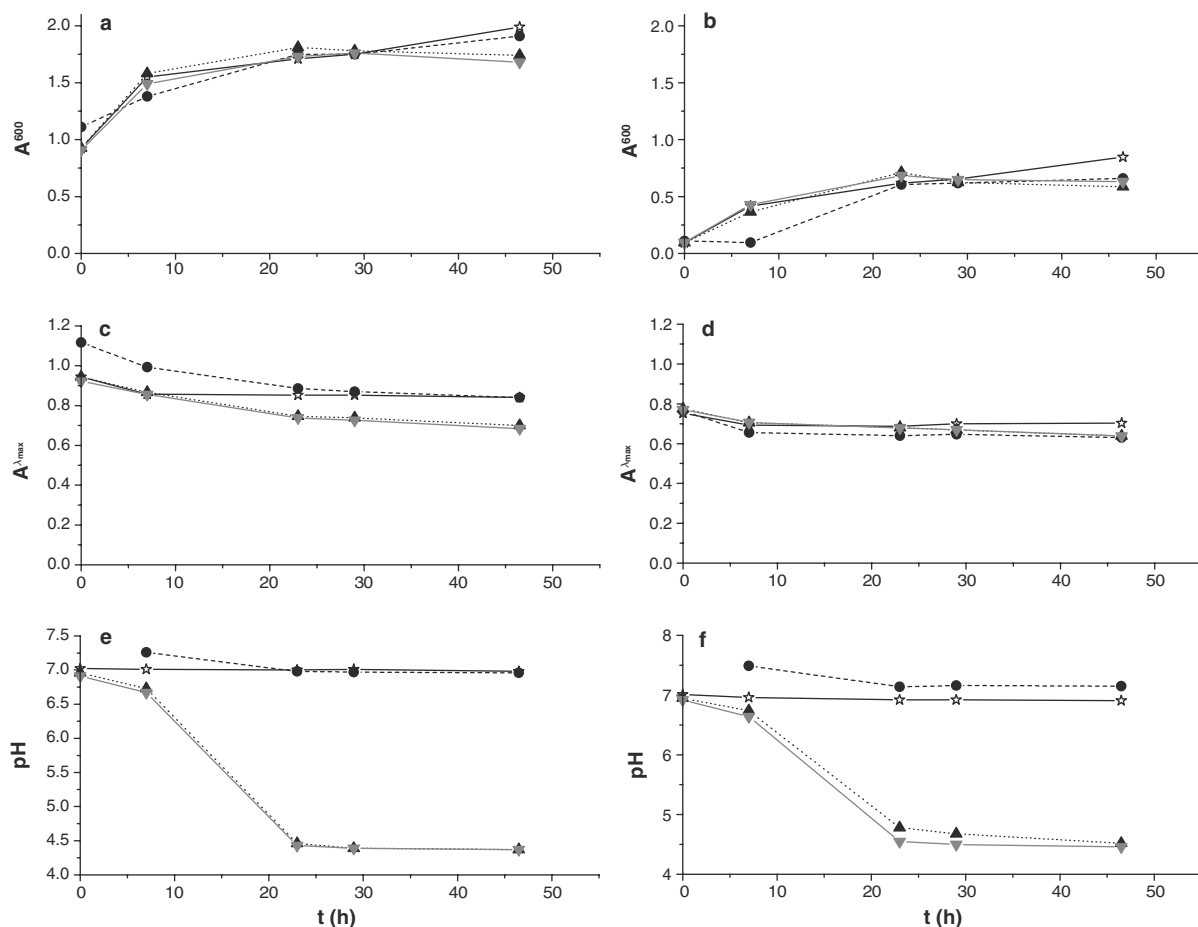


Fig. 2. Time-courses of turbidity (a and b), absorbance at λ_{max} (c and d) and pH (e and f) during growth of *Pseudomonas fluorescens* on the azo dyes RB5 (a, c and e) and RY145 (b, d and f) supplemented with 0 (\star , solid line), 1 (\bullet , dash line), 10 (\blacktriangle , dot line) and 20 (\blacktriangledown , solid line) g L⁻¹ glucose.

the 2 days of culture (Fig. 2a and b). Contrarily, at the end of culture on media containing 10 and 20 g L⁻¹ glucose, a weak decrease of the turbidity was recorded (Fig. 2a and b). This decline phase has to be related to the pH decrease only observed for 1% and 2% glucose supplementation of culture media (Fig. 2e and f). Indeed, after 1 day of growth, pH dropped to values close to 4.5, shown to be inhibitory for *P. fluorescens* [29]. The pH decrease was obviously not a consequence of ammonium assimilation, namely ammonium taken up in exchange for H⁺, lowering the pH of the culture medium [30]. Indeed, no pH decrease was observed during culture on media containing 0 or 1 g L⁻¹ glucose. The pH decrease was therefore most likely related to glucose consumption, leading to organic acids production; this assumption has to be subsequently confirmed. Inhibition by the pH led to an absence of nutritional limitations; total glucose consumption were similar, 6.2 and 6.6 g L⁻¹ were assimilated after 2 days of growth on media containing 10 and 20 g L⁻¹ glucose, respectively; and large amount of ammonium remained at the end of culture.

Following growth, RB5 biodegradation was higher than RY145 biodegradation. In absence of glucose, 11.0% and 6.5% of RB5 and RY145 were degraded (Fig. 2c and d); while the addition of glucose led to an increase of the biodegradation yield, which however appeared similar for all the glucose concentrations tested, 25.5 ± 0.6% and 17.5 ± 0.2% for RB5 and RY145 respectively (Fig. 2c and d). Even at low concentration, the presence of glucose favoured dye biodegradation, which was recorded throughout culture, while in absence of glucose the decrease of the absorbance at λ_{\max} was mainly recorded in the beginning of culture (Fig. 2c and d).

3.2. Integrated process

Owing to its lower biodegradability, the azo dye RY145 was chosen to test the integration of processes, photocatalysis and biological treatment.

Among the glucose supplementations tested, only the results recorded for 0 and 1% glucose were displayed. Indeed, 0.1% and 2% glucose led to similar results than those recorded for 0 and 1% glucose in the culture medium, respectively.

Three sets of runs were carried out. The ratio between the initial absorbance at λ_{\max} (419 nm) after the considered level of dye degradation and the non-photocatalysed solution were 0.70, 0.48 and 0, corresponding to 30%, 52% and 100% dye degradation, namely close to the theoretical values of 25%, 50% and 100% theoretical dye discoloration by photocatalysis. Indeed, the absorbances at λ_{\max} were 0.77 ± 0.01 (Fig. 2d), 0.54 ± 0.01 (Fig. 3d), 0.37 ± 0.01 (Fig. 3e) and 0 for IR0 (non-photocatalysed solution), IR25, IR50 and IR100 respectively.

Similarly to the changes observed in absence of an initial photocatalysis step, high initial rate of discoloration was recorded during *P. fluorescens* growth on the irradiated solutions IR25 and IR50, in absence of glucose in the culture medium, 7.8%, 25.3% and 23.6% for IR0, IR25 and IR50 respectively (Figs. 2d, 3d and e). The colouration remained then constant until the end of culture (Figs. 2d, 3d and e), confirmed by the results obtained in presence of 1 g L⁻¹ glucose (not shown). Similar initial discoloration rates were recorded in presence of 10 g L⁻¹ glucose, 9.0%, 25.1% and 19.8% for the solutions IR0, IR25 and IR50 respectively (Figs. 2d, 3d and e). High initial rates of discoloration, even in presence of a primary carbon source, agreed with the available literature [27,31]. Discoloration of the dye solution could be attributed to adsorption to the biomass and/or biodegradation [32,33]; the part played by each process may be subsequently examined by measuring the adsorption on dead cells. The further decrease recorded afterwards has to be most likely related to the pH decrease concomitantly recorded in presence of glucose, and can be therefore related to a change in the dye spectrum [27,32]. Consequently, measuring variations of absorbance at λ_{\max} have to be completed by the

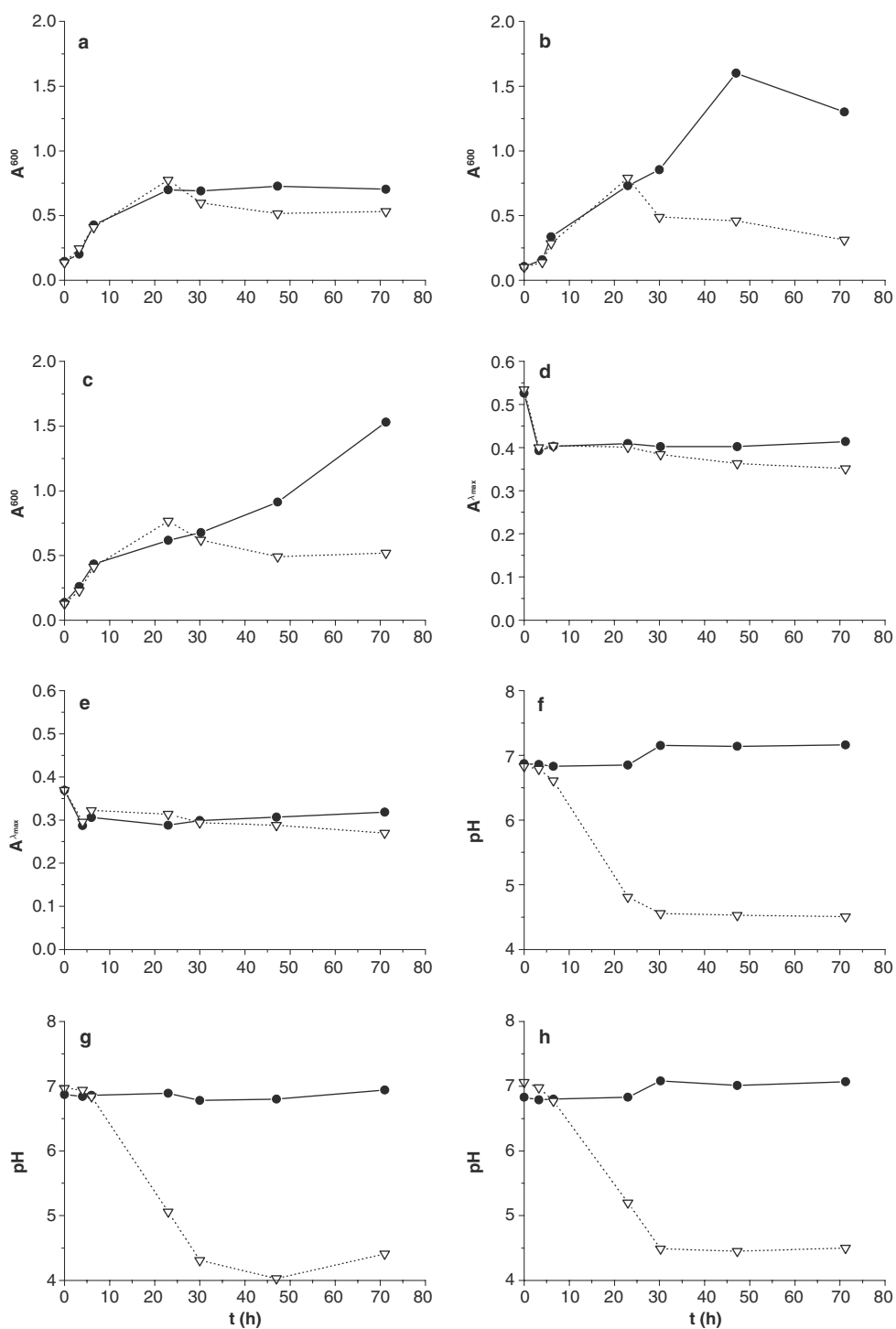


Fig. 3. Time-courses of turbidity (a, b and c), absorbance at λ_{max} (d and e) and pH (f, g and h) during growth of *Pseudomonas fluorescens* on a solution of the azo dye RY145 after 25 (a, d and f), 50 (b, e and g) and 100 (c and h) % of dye degradation by photocatalysis and supplemented with 0 (●, solid line) and 1 (▽, dot line) % glucose.

analysis of the visible colour spectrum [19,32]. Similarly to the data recorded in absence of a preliminary step of photocatalysis, the pH decrease resulting from glucose addition in the culture medium led to an inhibition of growth after less than 30 of culture, namely for pH close to 4.5 (Fig. 3f and h).

The significant growth recorded after total discolouration, namely 100% dye degradation by photocatalysis (RY100), should be noted (Fig. 3c). In absence of glucose addition, final turbidity was similar to that recorded for RY50 (Fig. 3b) and higher than the values recorded for RY0 (Fig. 2b) and RY25 (Fig. 3a) dye degradation by photocatalysis. In presence of glucose (1%), similar maximum turbidity values were recorded after the same culture time (1 day), owing to the inhibitory pH achieved (Fig. 3f and h). This showed that by-products released during the process of RY145 photodegradation could be, at least partially, assimilated by *P. fluorescens*. These results were confirmed by TOC measurements, since irrespective of the level of photocatalytic dye degradation, similar decrease of the TOC values were recorded during the subsequent cultures. Indeed, initial TOC values decreased from 584.0 to 509.7 mg L⁻¹ and final TOC values decreased from 225.4 mg L⁻¹ in absence of photocatalysis to 171.7 mg L⁻¹ after total photocatalytic dye degradation, respectively.

4. Conclusion

The feasibility of the use of an integrated process involving photocatalysis followed by biological treatment for dye degradation is confirmed. A biodegradation of the by-products resulting from the photocatalysis step was also shown. Identification of these intermediate by-products is in progress to propose a reaction pathway. Subsequent work have to be done to select the best microbial species for dye degradation, followed by integrated process optimisation to achieve

complete mineralisation of the considered azo dye at minimal cost.

References

- [1] S. Malato, J. Blanco, J. C aceres, A.R. Fernandez-Alba, A. Ag uera and A. Rodriguez, Photocatalytic treatment of water-soluble pesticides by photo-Fenton and TiO₂ using solar energy, *Catal. Today*, 76 (2002) 209–220.
- [2] S. Tanaka, K. Padermpole and T. Hisanaga, Photocatalytic degradation of commercial azo dyes, *Water Res.*, 34 (2000) 327–333.
- [3] C. Guillard, H. Lacheb, A. Houas, M. Ksibi, E. Elaloui and J.M. Herrmann, Influence of chemical structure of dyes, of pH and of inorganic salts on their photocatalytic degradation by TiO₂, comparison of the efficiency of powder and supported TiO₂, *J. Photochem. Photobiol. A: Chem.*, 158 (2003) 27–36.
- [4] C. Guillard, J. Disdier, C. Monnet, J. Dussaud, S. Malato, J. Blanco, M.I. Maldonado and J.M. Hermann, Solar efficiency of a new deposited titania photocatalyst: chlorophenol, pesticide and dye removal applications, *Appl. Catal. B: Environ.*, 46 (2003) 319–332.
- [5] U. Pagga and D. Brown, The degradation of dyestuffs — Part II: Behaviour of dyestuffs in aerobic biodegradation tests, *Chemosphere*, 15 (1986) 479–491.
- [6] A. Moutaouakkil, Y. Zeroual, F.Z. Dzayri, M. Talbi, K. Lee and M. Blaghen, Purification and partial characterization of azoreductase from *Enterobacter agglomerans*, *Archiv. Biochem. Biophys.*, 413 (2002) 139–146.
- [7] S. Sandhya, S. Padmavathy, K. Swaminathan, Y.V. Subrahmanyam and S.N. Kaul, Microaerophilic-aerobic sequential batch reactor for treatment of azo dyes containing simulated wastewater, *Process Biochem.*, 40 (2005) 885–890.
- [8] C.B. Shaw, C.M. Carliell and A.D. Wheatley, Anaerobic/aerobic treatment of coloured textile effluents using sequencing batch reactors, *Water Res.*, 36 (2002) 1993–2001.
- [9] K.T. Chung, G.E. Fulk and M. Egan, Reduction of azo dyes by intestinal anaerobes, *Appl. Environ. Microbiol.*, 35 (1978) 558–562.
- [10] G.M. Bonser, L. Bradshaw, D.B. Clayson and J.W. Jull, A further study on the carcinogenic

- properties of ortho-hydroxyamines and related compounds by bladder implantation in the mouse, *Br. J. Cancer*, 10 (1956) 539–546.
- [11] W. Delée, C. O'Neill, F.R. Hawkes and H.M. Pinheiro, Anaerobic treatment of textile effluents: a review, *J. Chem. Technol. Biotechnol.*, 73 (1998) 323–335.
- [12] W. Haug, A. Schmidt, B. Nörtemam, D.C. Hempel, A. Stolz and H.J. Knackmuss, Mineralisation of the sulphonated azo dye Mordant Yellow 3 by a 6-aminonaphthalene-2-benzenesulfonate-degrading bacterial consortium, *Appl. Microbiol. Biotechnol.*, 57 (1991) 3144–3149.
- [13] D. Méndez-Paz, F. Omil and J.M. Lema, Anaerobic treatment of azo dye Acid Orange 7 under batch conditions, *Enzyme Microb. Technol.*, 36 (2005) 264–272.
- [14] C.I. Pearce, J.R. Lloyd and J.T. Guthrie, The removal of colour from textile wastewater using whole bacterial cells: a review, *Dyes Pigments*, 58 (2003) 179–196.
- [15] S. Ledakowicz, M. Solecka and R. Zylla, Biodegradation, decolourisation and detoxification of textile wastewater enhanced by advanced oxidation processes, *J. Biotechnol.*, 89 (2001) 175–184.
- [16] M. Rodriguez, V. Sarria, S. Esplugas and C. Pulgarin, Photo-Fenton treatment of a biorecalcitrant wastewater generated in textile activities: biodegradability of the photo-treated solution, *J. Photochem. Photobiol. A: Chem.*, 151 (2002) 129–135.
- [17] V. Sarria, M. Deront, P. Péringer and C. Pulgarin, Degradation of a biorecalcitrant dye precursor present in industrial wastewaters by a new integrated iron(III) photoassisted-biological treatment, *Appl. Catal. B: Environ.*, 40 (2003) 231–246.
- [18] V. Sarria, S. Kenfack, O. Guillod and C. Pulgarin, An innovative coupled solar-biological system at field pilot scale for the treatment of biorecalcitrant pollutants, *J. Photochem. Photobiol. A: Chem.*, 159 (2003) 89–99.
- [19] N.P. Tantak and S. Chaudhari, Degradation of azo dyes by sequential Fenton's oxidation and aerobic biological treatment, *J. Hazard. Mat.*, 3 (2006) 698–705.
- [20] J.P. Scott and D.F. Ollis, Integration of chemical and biological oxidation processes for water treatment: review and recommendations, *Environ. Prog.*, 14 (1995) 88–103.
- [21] J.P. Scott and D.F. Ollis, Integration of chemical and biological oxidation processes for water treatment: II. Recent illustrations and experiences, *J. Adv. Oxid. Technol.*, 2 (1997) 374–381.
- [22] A.P. Trinci, A kinetic study of the growth of *Aspergillus nidulans* and other fungi, *J. Gen. Microbiol.*, 57 (1969) 11–24.
- [23] A. Aguedach, S. Brosillon, J. Morvan and E.K. Lhadi, Photocatalytic degradation of azo-dyes reactive black 5 and reactive yellow 145 in water over a newly deposited titanium dioxide, *Appl. Catal. B: Environ.*, 57 (2005) 55–62.
- [24] A.M. Cook, Biodegradation of *s*-triazine xenobiotics, *FEMS Microbiol. Lett.*, 46 (1987) 93–116.
- [25] D. Herbert, P.J. Phipps and R.E. Strange, Chemical analysis of microbial cells, in: J.R. Norris and D.W. Ribbons (Eds.), *Methods in Microbiology*, Vol. 5B, Academic Press, New York, 1971, pp. 265–308.
- [26] J. Rodier, Ammoniacal nitrogen analysis, in: *Water Analysis*, Vol. 1, Dunod, Paris, 1975, pp. 116–120.
- [27] M.S. Lucas, C. Amaral, A. Sampaio, J.A. Peres and A.A. Dias, Biodegradation of the diazo dye Reactive Black 5 by a wild isolate of *Candida oleophila*, *Enzyme Microb. Technol.*, 39 (2006) 51–55.
- [28] M.F. Mallette, Evaluation of growth by physical and chemical means, in: J.R. Norris and D.W. Ribbons (Eds.), *Methods in Microbiology*, Vol. 1, Academic Press, London, 1969, pp. 522–566.
- [29] L. Prescott, J. Harley and D. Klein, *Microbiologie*, 2nd edn., De Boeck, Bruxelles, 2003, 1137 pp.
- [30] J.W. Deacon, *Modern Mycology*, 3rd edn., Blackwell Science, Oxford, 1997, 303 pp.
- [31] P. Blaquez, N. Casas, X. Font, X. Gabarrell, M. Sarrà, G. Caminal and T. Vicent, Mechanism of textile metal dye biotransformation by *Trametes versicolor*, *Water Res.*, 38 (2004) 2166–2172.
- [32] F. Rigas and V. Dritsa, Decolourisation of a polymeric dye by selected fungal strains in liquid cultures, *Enzyme Microb. Technol.*, 39 (2005) 120–124.
- [33] T. Akar, T.A. Demir, I. Kiran, A. Ozcan, A.S. Ozcan and S. Tunali, Biosorption potential of *Neurospora crassa* cells for decolorization of Acid Red 57 (AR57) dye, *J. Chem. Technol. Biotechnol.*, 81 (2006) 1100–1106.